

Challenges related to standardized detection of crack initiation thresholds for lower-bound or ultra-long-term strength prediction of rock

E. Ghazvinian*, M. Diederichs* & J. Archibald†

*Dept. of Geological Sciences and Geological Engineering,
Queen's University, Kingston, Ontario, Canada

†Dept. of Mining Engineering, Queen's University, Kingston, Ontario, Canada



2011 Pan-Am CGS
Geotechnical Conference

ABSTRACT

Brittle spalling is a fracture mechanism that occurs in the walls of excavations in rocks with a low ratio of tensile to compressive strength. This mechanism does not always occur in laboratory strength tests. However, within a standard UCS test, it is possible to detect the onset of extensile damage accumulation and interaction. There are a number of methods to detect these thresholds involving either rigorous strain measurements or micro-acoustic monitoring. The Spall Prediction Commission of the International Society for Rock Mechanics is testing a number of processing algorithms for strain and acoustic data to develop a suggested methodology for crack initiation stress (CI) and crack interaction stress (CD) measurement. This paper examines both methods. A number of challenges with repeatable and reliable measurements of CI and CD are addressed and alternative approaches are proposed.

RÉSUMÉ

Écaillage fragile est un mécanisme de rupture qui se produit dans les murs de fouilles dans les roches avec un faible ratio de traction à la résistance à la compression. Ce mécanisme ne se produit pas toujours dans les tests de résistance en laboratoire. Toutefois, dans un test standard UCS, il est possible de détecter l'apparition de l'accumulation de dommages extensibles et l'interaction. Il ya un certain nombre de méthodes pour détecter ce seuils impliquant soit la souche rigoureuse mesure ou la surveillance micro-acoustique. La prévision Spall Commission de la Société internationale de mécanique des roches à l'essai un certain nombre d'algorithmes de traitement pour la souche et les données acoustiques de développer une méthodologie proposée pour le stress initiation de la fissure (CI) et le crack interaction stress (CD) de mesure. Cet article examine les deux méthodes. Une certain nombre de défis à la mesure reproductible et fiable de CI et de CD sont abordés et des approches alternatives sont proposées.

1 INTRODUCTION

Existing fractures in the rock tend to close as the in situ stress increases, due to increasing depth. This closure of the existing fractures in the rock makes the failure brittle (Martin et al 2001). The high induced compressive stresses around a deep opening result in the initiation and propagation of stress-induced fractures parallel to the excavation boundary (Figure 1).

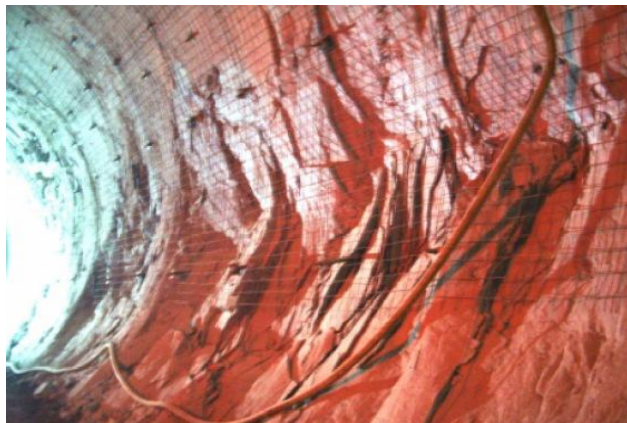


Figure 1. Stress-induced brittle failure around the Loetchberg tunnel, (Courtesy of M.S. Diederichs).

The stress magnitude around the underground opening plays a key role in the initiation and propagation of these stress-induced fractures. At the low and intermediate in situ stress levels, the stress magnitude may be just high enough to cause localized spalling and notch formation depending on the rock strength. However at greater depths the brittle failure may involve the whole boundary of the opening. The brittle failure mechanism around the underground openings is shown in Figure 2.

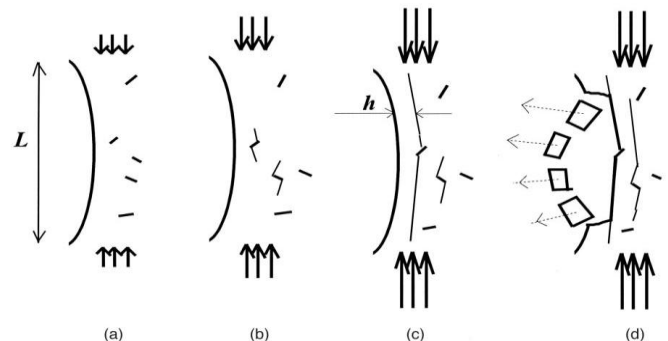


Figure 2. Development of brittle failure parallel to the excavation boundary due to the increase in the load. The rock would eventually fail after reaching the state (b), even with no increase in the axial stress, as the initial

cracks are formed and due to the absence of confining pressure they coalesce after some time (after Germanovich and Dyskin 1999).

As evident in Figure 2 the existing fractures start to extend and form wing cracks (Figure 3) parallel to the excavation surface in the absence of confining stress due to the increase in the stress magnitude around the excavation surface. The cracks propagate until they coalesce and start to interact. The interaction of the cracks causes slabbing and/or spalling around the opening boundary.

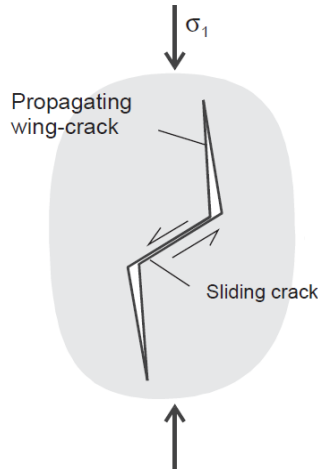


Figure 3. Extension of wing crack in the absence of confining stress (after Chandler 2004).

2 DAMAGE THRESHOLDS IN ROCKS

The crack initiation stress, CI, that corresponds to the extension crack damage threshold is shown in Figure 4 to be the in situ strength of the rock in low confinement. This threshold is a function of the nature and density of internal flaws and heterogeneity (Diederichs 2007). The damage initiation threshold is believed to be the long term (lower bound) in situ strength of the brittle rock. CI is the onset of non-linearity on the lateral strain–axial stress plot (Diederichs and Martin 2010). The short term or upper bound for the in situ strength of the brittle rock is the yield strength or the crack interaction strength (Diederichs 2007). The crack interaction strength, CD, which is the onset of non-linearity in axial stress-strain measurements, is the stress at which the cracks start to interact and coalesce. The International Society for Rock Mechanics (ISRM) Commission on Spalling Prediction is recommending the terminology of CI for crack initiation threshold and CD for crack interaction threshold (Diederichs and Martin 2010). These thresholds will be discussed further in this paper.

CI and CD thresholds are two important parameters that need to be determined for the design of underground excavations through laboratory testing. These parameters are used in the numerical codes for stability analyses and simulation of crack initiation, for instance defining the dimensions and fracture density within the EDZ. The

latter is a global topic of research and this study can contribute significantly to this research.

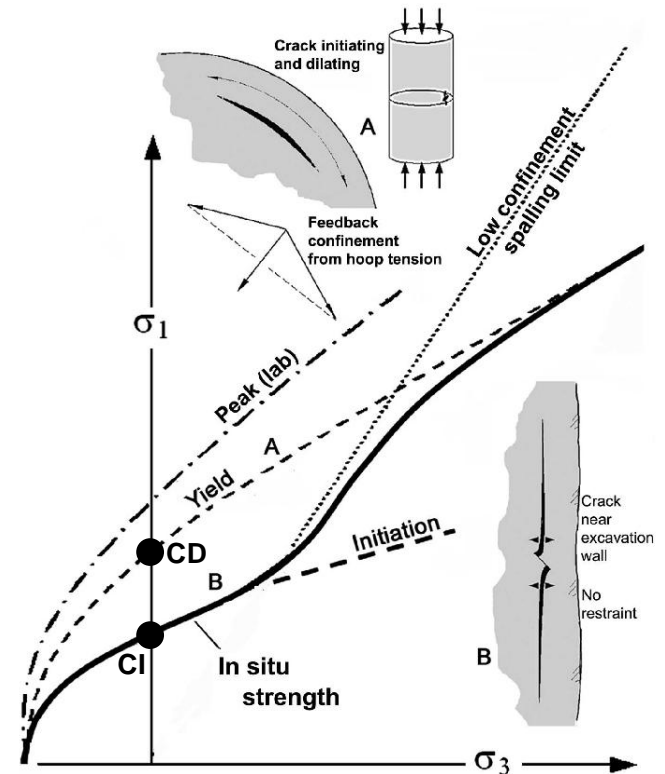


Figure 4. In situ yield envelope for brittle rocks, upper two dashed lines indicate conventional Hoek-Brown envelopes for yield and peak strength, damage initiation threshold is the long term strength of the rock under low confinement (after Diederichs 2007).

3 AVAILABLE METHODS FOR DAMAGE THRESHOLD ESTIMATION IN CRYSTALLINE ROCKS

Within a standard UCS test, it is possible to detect the onset of extensile damage accumulation. This threshold represents a lower bound for in situ wall strength of deep excavations in massive rock. There are a number of methods to detect this threshold involving either rigorous strain measurements or microseismic/acoustic emission monitoring. Crack initiation stress (CI), the lower bound for wall strength, manifests itself as an increase in lateral strain rate (for axial loading) and in a systematic increase in the rate of acoustic emissions (sound pulses) from the sample. In both cases, it is difficult to detect these thresholds from inspection of the raw data and some processing is required.

Different methods exist for detection of damage threshold levels i.e. CI (systematic damage) and CD (crack interaction). These methods can be categorized into two major methods of acoustic emission and strain measurement.

3.1 Acoustic emission method

In the acoustic emission (AE) method (Diederichs et al 2004), in which the cumulative number of AE events is plotted vs. stress, CI is the first point where the rate of crack emissions suddenly increases with a small change in load (Figure 5) and CD is where the subsequent sudden increase in the slope of the AE curve occurs (Diederichs 2007).

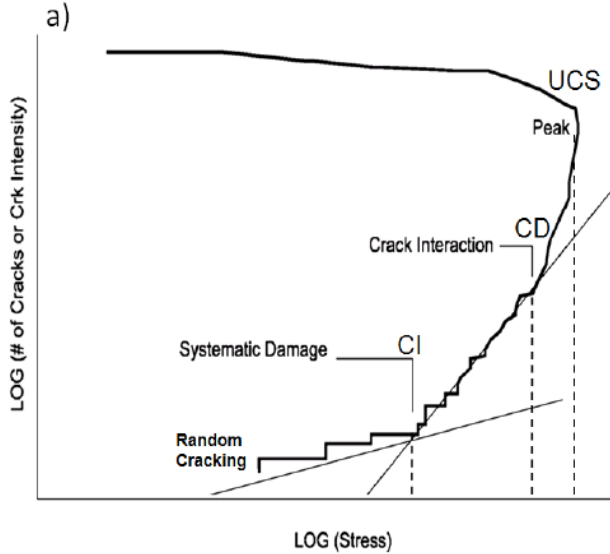


Figure 5. Damage detection using AE events (after Diederichs et al 2010).

3.2 Strain measurement method

For the strain measurement method different parameters can be used for estimation of CI and CD thresholds, calculated based on the measured axial and lateral strains. Crack volume strain and volumetric strain are the parameters that are widely being used for the estimation of CI and CD respectively.

3.2.1 Crack volume strain method for CI estimation

CI is defined as the stress where lateral strain, ϵ_l , departs from linearity (Figure 6). This non-linearity starts due to the cracks that begin to initiate all over the sample's volume (Eberhardt et al 1998). Crack-closure on the other hand is the point where closure of most cracks perpendicular to loading direction is observed and can be seen in the axial strain (ϵ_a). Both crack-closure anomalies and damage initiation in rocks can be captured by lateral strain. Therefore when crack-closure and crack initiation limits overlap in the lab data, the interpretation of CI gets more complex as both crack-closure and crack initiation limits have an effect on the lateral strain plot. This overlap generally occurs for the samples that are damaged prior to testing. To prevent this problem Martin (1994) and Diederichs and Martin (2010) suggested the reversal point of crack volumetric strain (ϵ_{CV}) as the CI threshold (Figure 6). Crack volumetric strain can be calculated as follows;

$$\epsilon_{CV} = \epsilon_{VOL} - \epsilon_{EV} \quad [1]$$

where: ϵ_{VOL} = Volumetric strain
 ϵ_{EV} = Elastic volumetric strain

ϵ_{VOL} and ϵ_{EV} are calculated as follows;

$$\epsilon_{VOL} = \epsilon_a + 2\epsilon_l \quad [2]$$

and;

$$\epsilon_{EV} = \left(\frac{\sigma}{E}\right)(1 - 2\nu) \quad [3]$$

Based on Equation 3 the elastic volumetric strain is dependent upon the Poisson's ratio and Young's modulus. In some cases the accurate estimation of these parameters to a constant value is difficult or impossible in damaged rocks.

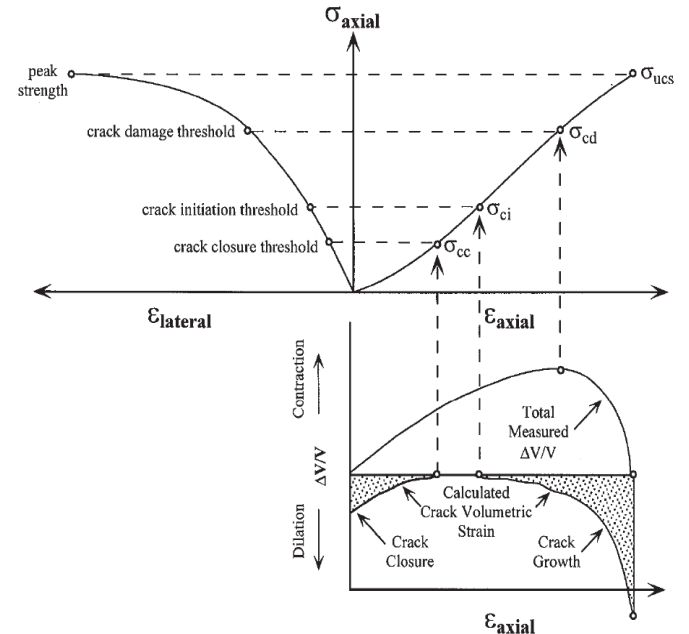


Figure 6. Damage progress in brittle rocks (after Martin 1994).

3.2.2 Volumetric strain method for CD estimation

The reversal point of total measured volumetric strain (ϵ_{VOL}) was suggested by Martin (1997) to be representative of CD threshold (Figures 6). Alternatively, Diederichs (2003, 2007) showed that the volumetric strain reversal point is not representative of CD in confined samples. This is due to the fact that in higher confining pressures the time that lateral strain starts to accelerate is coincidental with an increase in the vertical strain rate and as volumetric strain is the summation of lateral and axial strains, the reversal of this curve is delayed until a considerable increase in the rate of lateral strain occurs. The volumetric strain is calculated using equation 2.

3.2.3 Introducing new parameter for CI estimation based on measured strains: Tangent lateral stiffness

As previously stated in Section 3.2.1, lateral strain captures both crack-closure anomalies and damage initiation. Therefore in the case of overlapping crack-closure and crack initiation limits, it will be hard to distinguish between the two. To avoid the problem of crack-closure and crack initiation overlap and to reduce the subjectivity of picking the point where non-linearity begins, the inverse tangent lateral stiffness has been proposed by the authors as a potential solution. Inverse tangent lateral stiffness is calculated by using Equation 4;

$$\varepsilon_l \Delta = \frac{\Delta \varepsilon_l}{\Delta \sigma} \quad [4]$$

where; $\Delta \sigma = \sigma_{i+8} - \sigma_{i-8} \text{ (} i = 1, 2, 3, 4, \dots \text{)}$
 $\Delta \varepsilon_l = \varepsilon_{l i+8} - \varepsilon_{l i-8} \text{ (} i = 1, 2, 3, 4, \dots \text{)}$

Identification of CI by using the inverse tangent lateral stiffness for a sample of Smaland granite and a sample of Stanstead granite has been shown in Figures 12 and 16 respectively. As evident in Figures 12 and 16 with a good choice of scale for the graph, CI can be picked quite accurately at the inflection point of the curves.

3.2.4 Introducing new parameter for CD estimation based on measured strains: Tangent modulus

The deviation in Young's modulus has not been used widely in rock mechanics for damage detection unlike other fields such as civil or mechanical engineering. "Tangent modulus" that is the moving average of Young's modulus is calculated as follows;

$$E \Delta = \frac{\Delta \sigma}{\Delta \varepsilon_a} \quad [5]$$

where: $\Delta \sigma = \sigma_{i+3} - \sigma_{i-3} \text{ (} i = 1, 2, 3, 4, \dots \text{)}$
 $\Delta \varepsilon_a = \varepsilon_{a i+3} - \varepsilon_{a i-3} \text{ (} i = 1, 2, 3, 4, \dots \text{)}$

Tangent modulus will be further explored in the next few sections of the paper based on the testing data of Smaland and Stanstead granites.

4 LABORATORY TESTING RESULTS

Eight UCS samples of Stanstead granite were tested under uniaxial loading for this study. The ISRM SM for the complete stress-strain curve for intact rock in uniaxial compression (ISRM 1999) were followed and applied for both sample preparations and testing.

Specimens were monitored by both the strain measurement sensors (strain gauges (Figure 7) and LVDTs (for axial deformation)) and Acoustic Emission system (Figure 8) to collect data for both strain measurement and AE methods. Rosette strain gauges were used for measuring axial and lateral strains. Gauges with a length of 10 mm and with a gauge factor of 2.12 were used. Prior to gluing the strain gauges in place, the surfaces of the specimens were cleaned using contact cleaner. Gauges were bonded at the mid height of the

samples. All tests were monitored with AE system, using the four AE transducers. The transducers were mounted mid height on the sample, slightly above the strain gauges at a 90 degree orientation from each other. Honey was used as a couplant and the transducers were kept in place with a rubber band. Example for a specimen before the test is shown in Figure 9.

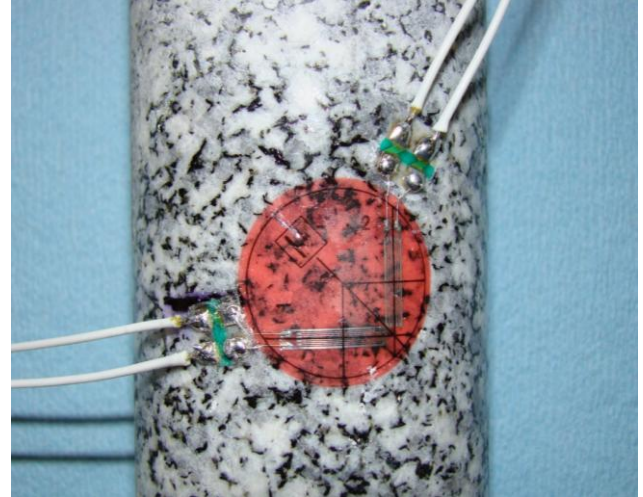


Figure 7. Rosette strain gauges were used for the measurement of axial and lateral strains of Stanstead granite samples.



Figure 8. AE transducer (circle) and pre-amplifier used for AE monitoring.

The authors were presented with high quality data of UCS testing of Smaland granite (Figure 10) from Forsmark, Sweden (courtesy of ISRM Commission on Spalling Prediction, CANMET and SKB). Extensive analysis on the Stanstead granite and Smaland granite test results has been done to gain a better understanding of using strain measurement values and Acoustic Emission data for detecting damage thresholds (CI, CD) in brittle rocks. In this regard, a high quality set of UCS testing data on Smaland granite was used to highlight the strengths and weaknesses of different methods for detecting damage limits in granitic rocks.

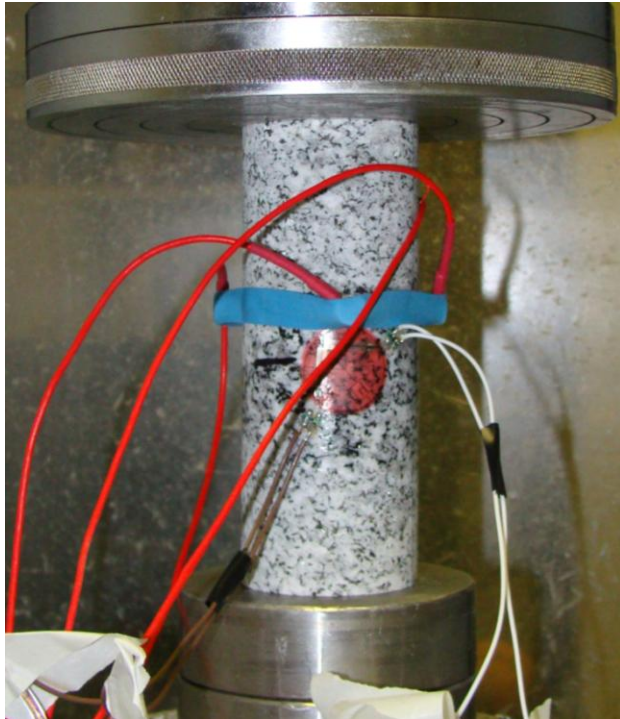


Figure 9. A Stanstead granite specimen ready for testing.



Figure 10. A Smaland granite specimen ready for testing, the specimen was monitored by AE sensors, vertical and horizontal strain gauges, LVDTs for axial deformation and extensometer for circumferential strain (Courtesy of ISRM Commission on Spalling Prediction).
4.1 Smaland granite

In Figure 11 the Log “cumulative AE counts” versus Log “stress” was plotted for a sample of Smaland granite. The first point where the slope of the AE curve rapidly changes is identified as CI. The onset of CI threshold can be identified with high accuracy within a short range in Figure 11. The CD threshold can be detected accurately where the second change in the slope of AE curve occurs. As seen in Figure 11 the range for CD is very small.

The crack counts that are shown in Figure 11 as AE data are the cumulative number of cracks (AE events) averaged from multiple AE transducer readings (Diederichs et al 2004, Eberhardt et al 1999).

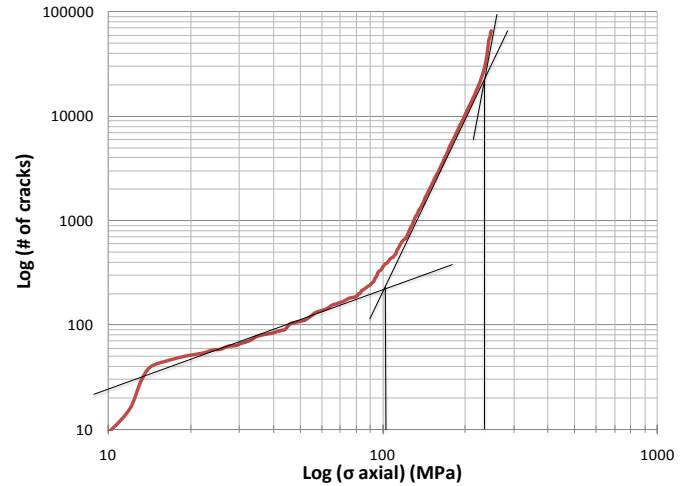


Figure 11. Detection of CI and CD by using AE method for the Smaland granite sample.

The identification of CI using the inverse tangent lateral stiffness for the sample of Smaland granite is shown in Figure 12. CI can be picked quite accurately at the inflection point of the curve as shown in this figure.

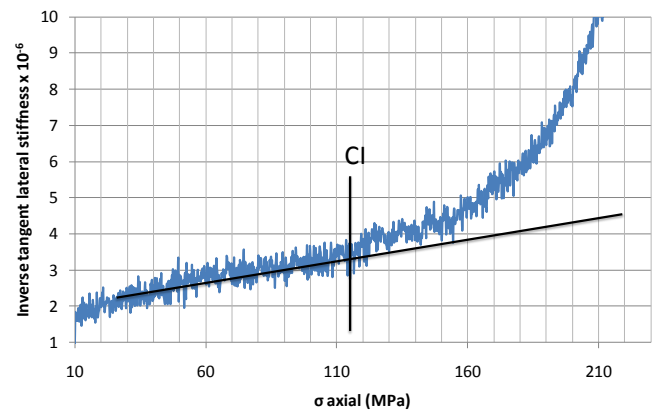


Figure 12. Detection of CI for the Smaland granite using inverse tangent lateral stiffness.

Crack volumetric strain and volumetric strain versus stress, have been plotted for the Smaland granite sample in Figures 13. CI and CD thresholds can be picked at the reversal point of the crack volumetric strain and the volumetric strain curves respectively.

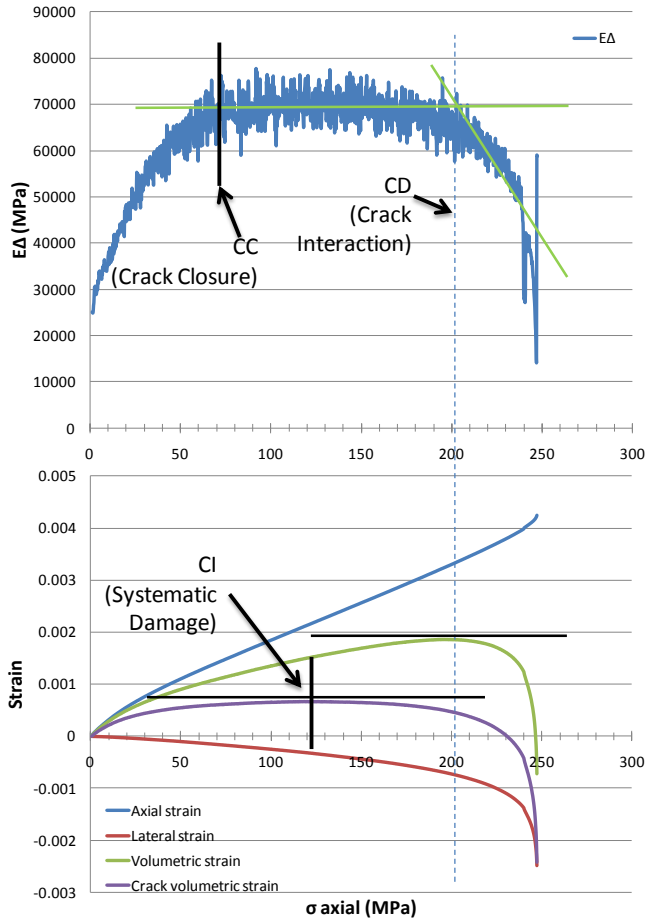


Figure 13. Detection of CI and CD for the Smaland granite sample using tangent modulus ($E\Delta$), volumetric strain and crack volume strain methods.

Figure 13 illustrates how the tangent modulus ($E\Delta$) starts to behave like a linear elastic material after a steady increase. This is the onset of the crack closure limit in rock as most of the cracks non-parallel to loading are closed, resulting in a maximum tangential stiffness. After this limit the samples start to behave linearly in terms of axial stiffness. New cracks initiate parallel to the loading direction and are not detected in $E\Delta$ plot. As soon as the density of cracks in the sample reaches a certain limit that is large enough for cracks to coalesce and interact, the slope of the tangent modulus start to decrease. Therefore the second slope change in the tangent modulus curve can be used for detection of CD.

4.2 Stanstead granite

All the methods that have been mentioned in Section 3 for detection of CI and CD thresholds, are applied to a UCS sample of the Stanstead granite. The results for the sample of Stanstead granite are shown in Figures 14, 15 and 16. Identification of CI and CD thresholds from the application of AE method for the Stanstead granite sample is shown to be well defined in Figure 14.

Overlapping of the crack closure and systematic damage thresholds can be interpreted from the tangent

modulus curve in Figure 15 for the Stanstead granite sample. The late arrival of the tangent modulus into an approximate linear elastic behaviour, which is the state that new cracks start to form randomly in the sample, shows the severity of damage in the sample prior to testing.

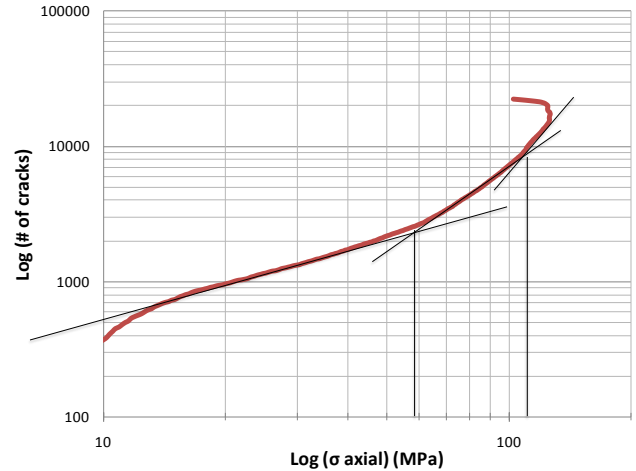


Figure 14. Detection of CI and CD by using AE method for the Stanstead granite sample.

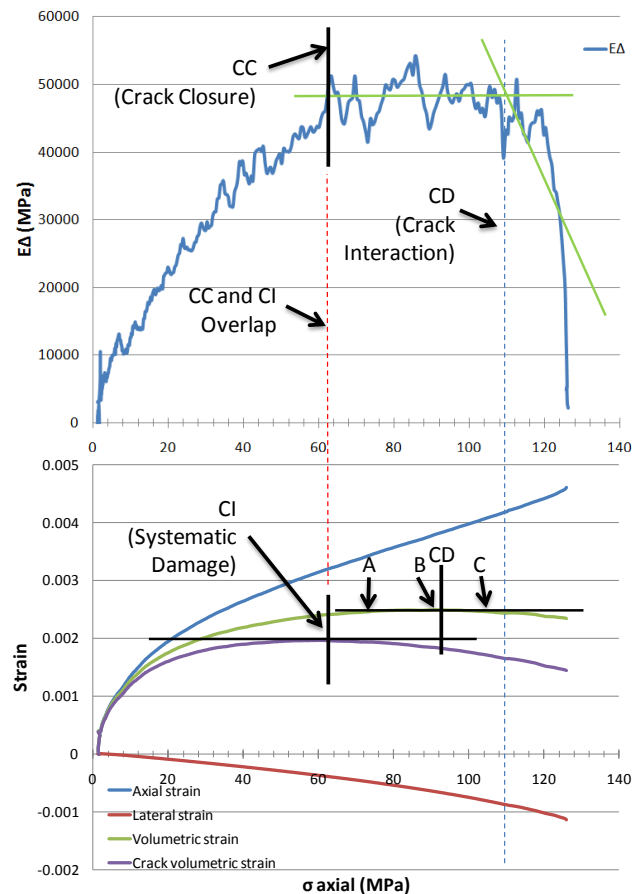


Figure 15. Detection of CI and CD for the Stanstead granite sample using tangent modulus ($E\Delta$), volumetric strain and crack volume strain methods.

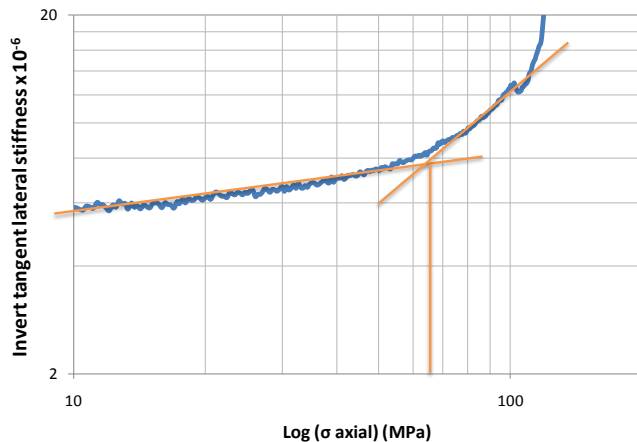


Figure 16. Detection of CI for the Stanstead granite using inverse tangent lateral stiffness.

For estimating the CD threshold, both the tangent modulus and volumetric strain have been plotted in the same figure (Figures 15). It can be seen that the slope change in the tangent modulus method provides a clear point associated with the stress value corresponding to CD, while the point where the dilation begins, in the volumetric strain, is not as obvious. In the volumetric strain method the question arises as to which point should be picked as the starting point of dilation? Is it the point where the curve's slope starts to decrease (point A in Figure 15), the curve reversal point (point B in Figure 15) or the point where volumetric strain slope tends to increase (point C in Figure 15) and what will be the answer in case of a flat maximum for volumetric strain curve. This wide range of possible CI values, when using the volumetric strain method, makes this method less favourable than the inverse tangent modulus method.

For CI threshold determination, crack volume strain for the Stanstead granite sample is plotted in Figure 15. The inverse of the tangent lateral stiffness is plotted in Figure 16. In crack volume strain method picking a point by using reversal of a curve is associated with similar difficulties as mentioned for CD detection using the volumetric strain method. The high sensitivity of the crack volume strain to the Poisson's ratio is the another drawback to this method. The process of calculating Poisson's ratio is subjective by itself due to its variability depending on the interval chosen for calculation of Poisson's ratio. This will be discussed further on the Smaland granite sample in Section 5. The other uncertainty associated with the crack volume strain method is the error caused in the case of overlapping crack closure with the onset of CI. The inverse of tangent lateral stiffness provides the onset of CI threshold quite clearly, at the point of slope change, in spite of having previously damaged samples. This is because the method is detecting the rate of change in the slope of the lateral stiffness, which is an inflection point independent of the sample behaviour.

5 VARIABILITY OF DIFFERENT THRESHOLD DETECTION METHODS

The CD value detected for the Smaland granite sample in Figure 13 by using the tangent modulus corresponds relatively well to the volumetric strain method but it is not aligned exactly with the reversal point of the volumetric strain curve. The concept behind identifying the reversal point of the volumetric strain curve as the CD threshold is that the lateral strain surpasses the axial strain as the dominant parameter in volumetric strain. The authors are of the opinion that this concept can be useful for finding a range for CD, but finding a specific CD value, with a very small range, is not always possible, especially when the curve has a flat maximum.

The reversal point of crack volumetric strain for the Smaland granite sample is shown in Figure 13 for detection of the CI threshold. All the difficulties and errors associated with identifying the reversal point of a curve that have been discussed for CD are applicable for CI as well. The errors are even larger for CI, as the crack volume strain normally has a much flatter curvature at the maximum compared to the volumetric strain plot. For instance in Figure 12 the CI can be picked anywhere in the range of 100 to 140 MPa.

The high sensitivity of crack volume strain to the Poisson's ratio (Eberhardt et al 1998) is another problem associated with this method for detecting CI. The high variability of Poisson's ratio itself, due to the interval that is being picked for calculation of Poisson's ratio, introduces a high degree of uncertainty to the crack volume strain. Figure 17 shows the plot for the incremental crack volume strain, which is the difference between every six neighbouring data points. This graph shows the change in the slope of crack volume strain. The point where incremental crack volume strain crosses the x axis approximately shows the reversal point of the crack volume strain curve (CI). Incremental crack volume strain curves have been plotted for three different Poisson's ratios. It can be seen that by increasing the Poisson's ratio from 0.2 to 0.4 it can cause about 60 to 70 MPa increase for the CI limit.

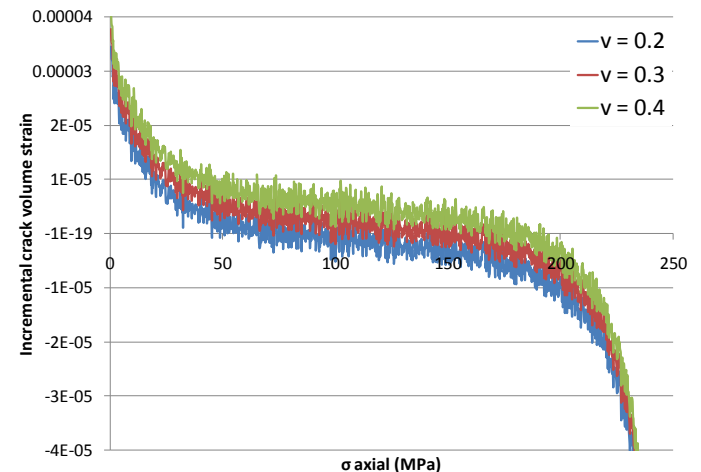


Figure 17. Incremental crack volume strain for the Smaland granite sample based on three Poisson's ratio of 0.2, 0.3 and 0.4.

Based on what has been discussed so far, the methods in which the damage thresholds are identified from the sudden change in the slope of curves seem to be more accurate than the curve reversal methods, especially in reversals that happen very gradually.

6 CONCLUSIONS

Comparing all the methods discussed in this paper for detecting damage thresholds in a granitic rock, the AE method was the most robust method that could estimate the threshold levels accurately, even in a previously damaged sample. The strain measurement method was less successful due to the larger difference between the lower and upper bound detected for CI and CD in most cases. Using the measured strains, the tangent lateral stiffness method used for detecting CI was in good agreement with the AE method results and much more accurate than the crack volume strain method. The strain measurement method can be more accurate when using extensometers for measuring axial and lateral strains instead of electrical resistivity strain gauges. This is due to the fact that strain gauges can only cover several grains (approximately 3 grains in the case of the Stanstead granite) and these grains may not be representative of the global behaviour of the sample.

ACKNOWLEDGEMENTS

The authors would like to thank NSERC and NWMO for their financial support. The authors would also like to acknowledge ISRM Commission on Spalling Prediction, SKB and Canmet for providing the testing data of the Smaland granite.

REFERENCES

- Chandler, N. 2004. Developing tools for excavation design at Canada's Underground Research Laboratory. *Int. J. Rock Mech. Min. Sci.* 41, 1229-1249.
- Diederichs, M.S. 2003. Rock fracture and collapse under low confinement conditions. *Rock Mechanics and Rock Engineering.* 36(5), 339-381.
- Diederichs, M.S. 2007. The 2003 CGS geocolluquium address: Damage and spalling prediction criteria for deep tunnelling. *Can. Geotech. J.* 44(9), 1082-1116.
- Diederichs, M.S. Carter, T. Martin, D. 2010. Practical rock spall predictions in tunnels. *Proc. World Tunnel Congress 2010.* Vancouver, Canada.
- Diederichs, M.S. Kaiser, P.K. Eberhardt, E. 2004. Damage initiation and propagation in hard rock tunnelling and the influence of near-face stress rotation. *Int. J. Rock Mech. Min. Sci.* 41, 785-812.
- Diederichs, M.S. Martin, C.D. 2010. Measurement of spalling parameters from laboratory testing. *Proc. Eurock 2010,* Lausanne, Switzerland.
- Eberhardt, E. Stead, D. Stimpson, B. 1999. Quantifying progressive pre-peak brittle fracture damage in rock during uniaxial compression. *Int. J. Rock Mech. Min. Sci.* 36, 361-380.
- Eberhardt, E. Stead, D. Stimpson, B. and Read, R.S. 1998. Identifying crack initiation and propagation thresholds in brittle rock. *Canadian Geotechnical Journal,* 35 (2), 222-233.
- Germanovich, L.N. Dyskin, A.V. 2000. Fracture mechanisms and instability of openings in compression. *Int. J. Rock Mech. Min. Sci.* 37, 263-284.
- International Society for Rock Mechanics Commission on Standardization of Laboratory and Field Tests. 1999. Suggested method for the complete stress-strain curve for intact rock in uniaxial compression. *Int. J. Rock Mech. and Min. Sci.* 36, 279-289.
- Martin, C.D. 1994. *The Strength of Massive Lac du Bonnet Granite around Underground Openings.* Ph.D. Thesis. University of Manitoba.
- Martin, C.D. 1997. Seventeenth Canadian Geotechnical Colloquium: The effect of cohesion loss and stress path on brittle rock strength. *Can. Geotech. J.,* 34 (5), 698-725.
- Martin, C.D. Christiansson, R. Soderhall, J. 2001. Rock stability considerations for siting and constructing a KBS-3 repository based on experiences from Aspö HRL, AECL's URL, tunnelling and mining. *Technical Report TR-01-38,* SKB.